



Article

# The ABCG2 Transporter Affects Plasma Levels, Tissue Distribution and Milk Secretion of Lumichrome, a Natural Derivative of Riboflavin

Alicia Millán-García , Laura Álvarez-Fernández , Esther Blanco-Paniagua , Ana I. Álvarez and Gracia Merino \*

Department of Biomedical Sciences–Physiology, Faculty of Veterinary Medicine, Animal Health Institute (INDEGSAL), Campus de Vegazana, Universidad de León, 24071 León, Spain; amilg@unileon.es (A.M.-G.); lalvf@unileon.es (L.Á.-F.); eblap@unileon.es (E.B.-P.); aialvf@unileon.es (A.I.Á.)  
\* Correspondence: gmerp@unileon.es

**Abstract:** The ABCG2 membrane transporter affects bioavailability and milk secretion of xenobiotics and natural compounds, including vitamins such as riboflavin. We aimed to characterize the in vitro and in vivo interaction of ABCG2 with lumichrome, the main photodegradation product of riboflavin, which has proven in vitro anti-cancer activity and a therapeutical role in antibacterial photodynamic therapy as an efficient photosensitizer. Using MDCK-II polarized cells overexpressing murine *Abcg2* and human ABCG2 we found that lumichrome was efficiently transported by both variants. After lumichrome administration to wild-type and *Abcg2*<sup>-/-</sup> mice, plasma AUC<sub>20–120 min</sub> was 1.8-fold higher in *Abcg2*<sup>-/-</sup> mice compared with wild-type mice. The liver and testis from *Abcg2*<sup>-/-</sup> mice showed significantly higher lumichrome levels compared with wild-type, whereas lumichrome accumulation in small intestine content of wild-type mice was 2.7-fold higher than in *Abcg2*<sup>-/-</sup> counterparts. Finally, a 4.1-fold-higher lumichrome accumulation in milk of wild-type versus *Abcg2*<sup>-/-</sup> mice was found. Globally, our results show that ABCG2 plays a crucial role in plasma levels, tissue distribution and milk secretion of lumichrome potentially conditioning its biological activity.

**Keywords:** lumichrome; flavor; ABCG2; plasma levels; tissue distribution; milk secretion



**Citation:** Millán-García, A.; Álvarez-Fernández, L.; Blanco-Paniagua, E.; Álvarez, A.I.; Merino, G. The ABCG2 Transporter Affects Plasma Levels, Tissue Distribution and Milk Secretion of Lumichrome, a Natural Derivative of Riboflavin. *Int. J. Mol. Sci.* **2024**, *25*, 9884. <https://doi.org/10.3390/ijms25189884>

Academic Editors: Lorena Pochini and Tiziano Mazza

Received: 2 August 2024

Revised: 30 August 2024

Accepted: 12 September 2024

Published: 13 September 2024



**Copyright:** © 2024 by the authors. Licensee MDPI, Basel, Switzerland. This article is an open access article distributed under the terms and conditions of the Creative Commons Attribution (CC BY) license (<https://creativecommons.org/licenses/by/4.0/>).

## 1. Introduction

One of the key mechanisms that affects biodistribution and milk secretion of natural compounds and xenobiotics is the ATP-binding cassette transporter G2 (ABCG2), also known as breast cancer resistance protein (BCRP). It is expressed in the apical membrane of cells of organs that play a relevant role in biodistribution of compounds, such as the liver, kidney and gastrointestinal tract; the blood–brain, blood–placental and blood–testis barriers; and the lactating mammary gland [1,2]. It behaves as an efflux pump, playing a xenobiotic protective role in individual cells, in some organs and in the body as a whole [1,3]. Moreover, it modulates the absorption, distribution and elimination of drugs and natural and endogenous compounds [4,5], conditioning its pharmacokinetics and tissue distribution, lessening plasma levels of its substrates [1]. It is worth noting that it is the only ABC transporter that participates in the secretion of its substrates into milk [6].

Lumichrome, the main product of the photodegradation of riboflavin (vitamin B<sub>2</sub> or lactoflavin) [7–10], is a natural compound present in the human body [11–13]. Coming from several sources, it is synthesized from riboflavin in the liver, kidney and digest-free small intestine [14] and produced by intestinal bacteria as a byproduct of the metabolism of riboflavin [15]. Out of the body, it can be efficiently produced by different microorganism strains such as *Microbacterium* sp. [16], *Pseudomonas riboflavina* [17], marine sponge-associated fungus *Acremonium persicinum* [18] and a species of *Nocardia* [19]. It can also be

chemically synthesized [20,21] or synthesized by photodegradation of riboflavin in neutral or acidic conditions [8,11,22,23].

Regarding its biological effects, it is a nontoxic molecule [13,24] which acts as a competitive flavin reductase inhibitor [25,26]. Although the inhibition of this enzyme may interfere in the *in vitro* reduction of methaemoglobin to haemoglobin, it is believed that under normal conditions the enzyme scarcely contributes to that process [27].

It also inhibits, in a concentration-dependent manner, the riboflavin uptake by riboflavin carriers in HepG2 cells [28]. Additionally, it plays a therapeutic role in antibacterial photodynamic therapy as an efficient photosensitizer [11,29].

Lumichrome has proven anti-cancer activity in non-small-cell lung cancer (NSCLC) cell lines by suppressing growth and inducing apoptosis through p53-dependent mechanisms at concentrations above 25  $\mu\text{M}$  [30]. It also shows significant cytotoxic activity against liver, breast and colorectal cancer cell lines (HepG2, MCF-7 and Colo-205, respectively), at concentrations higher than 40  $\mu\text{M}$  [31].

In the presence of light, lumichrome efficiently produces singlet oxygen species [9], which induce the oxidation of sulfur-containing proteins and polyunsaturated fatty acids, [32,33] producing undesirable impairment of the sensorial properties of milk [34]. This may reduce milk nutritional value, making it unacceptable to consumers [35], since the sensorial characteristics of milk products are directly related to milk quality [36].

Riboflavin, the lumichrome precursor, is an *in vitro* and *in vivo* substrate of murine Abcg2 [37]. However, *in vitro* and *in vivo* interactions of ABCG2 with lumichrome remain unknown. Consequently, the aim of this study was to evaluate whether lumichrome is an *in vitro* substrate of ABCG2 and to describe the role of ABCG2 in plasma levels, tissue distribution and milk secretion of the aforementioned compound.

## 2. Results

### 2.1. Murine Abcg2 and Human ABCG2 Efficiently *In Vitro* Transport Lumichrome

To assess the role of ABCG2 in the *in vitro* transport of lumichrome, the MDCK-II parental cell line and its subclones transduced with murine Abcg2 and human ABCG2 were used, and vectorial transport of lumichrome across the monolayer was determined and relative efflux ratios were calculated (Figure 1, Table 1). The MDCK-II parental cell line displayed a similar transport pattern in either direction, apical to basolateral (AB) and basolateral to apical (BA) (Figure 1A,C,E), which is reflected in the relative efflux transport ratio (BA/AB) at 4 h ( $0.85 \pm 0.13$ ). However, murine Abcg2 and human ABCG2 subclones presented not only a higher basolateral to apical transport but also a lower apical to basolateral transport compared with parental cells, which resulted in significantly higher relative efflux transport ratios of  $13.81 \pm 3.25$  ( $p < 0.001$ ) and  $2.57 \pm 0.25$  ( $p < 0.001$ ), respectively.

**Table 1.** Relative efflux transport ratio (apically directed translocation percentage divided by basolaterally directed translocation percentage) at 4 h for lumichrome (10  $\mu\text{M}$ ) in parental MDCK-II cells and their subclones transduced with murine (mAbcg2) or human ABCG2 (hABCG2) variant, either in the absence (−Ko143) or the presence of the ABCG2-specific inhibitor Ko143 (1  $\mu\text{M}$ ) ( $n \geq 3$ ).

	−Ko143	+Ko143
MDCK-II	$0.85 \pm 0.13$	$0.95 \pm 0.03$
MDCK-II mAbcg2	$13.81 \pm 3.25^*$	$1.03 \pm 0.04$
MDCK-II hABCG2	$2.57 \pm 0.25^*$	$1.08 \pm 0.08$

Results are shown as mean  $\pm$  S.D. (\*)  $p \leq 0.05$ : significant differences in transport ratio compared with parental MDCK-II cells.

The specificity of vectorial transport was checked using a specific inhibitor of ABCG2, Ko143. ABCG2-mediated transport was completely inhibited in all subclones (Figure 1B,D,F) which was reflected in similar relative efflux transport ratios between parental and transduced cells. These results show that lumichrome is efficiently transported by murine and human variants of the ABCG2 transporter.

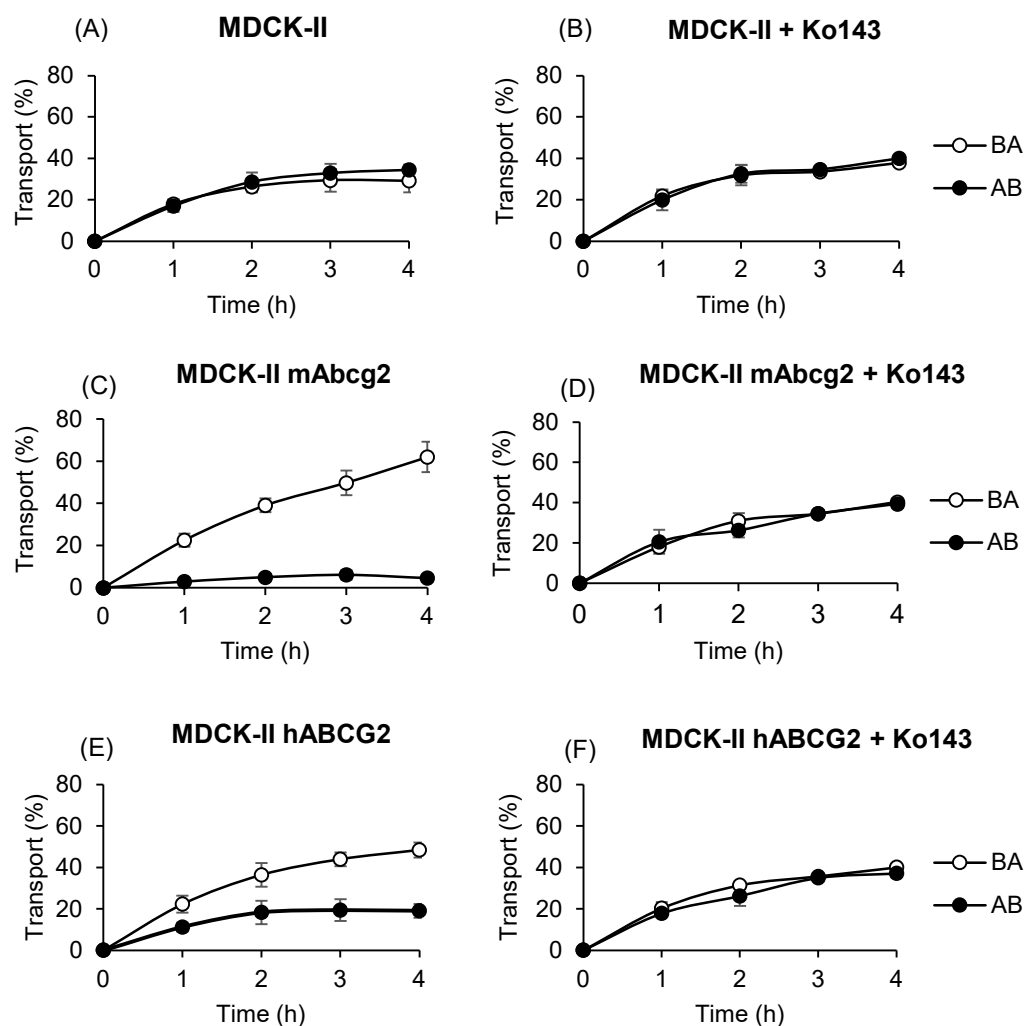


**Figure 1.** Transepithelial transport assay of lumichrome (10  $\mu$ M) with or without the ABCG2-specific inhibitor Ko143 (1  $\mu$ M) in parental MDCK-II cells (A,B) and their subclones transduced with murine (C,D) and human (E,F) ABCG2 variants. The experiment began by replacing the medium of both compartments with fresh culture medium with or without inhibitor and containing 10  $\mu$ M lumichrome. Aliquots were taken at 1, 2, 3 and 4 h on the opposite side to where lumichrome had been added. All samples were stored at  $-20$   $^{\circ}$ C until being analyzed by HPLC. Lumichrome appearance in the opposite compartment was presented as the fraction of the total compound added at the beginning of the experiment and expressed as a percentage. Results are shown as mean  $\pm$  S.D.

## 2.2. Plasma Levels and Tissue Distribution of Lumichrome in Wild-Type and *Abcg2*<sup>-/-</sup> Male Mice

To also evaluate the extent to which in vitro transport of lumichrome mediated by ABCG2 is reflected in vivo, plasma and tissue levels of lumichrome were measured in wild-type and *Abcg2*<sup>-/-</sup> male mice after its intraperitoneal administration at a dose of 10 mg/kg. This setting was selected rooted in previous studies, where sham-operated or ovariectomized female mice were intraperitoneally injected with lumichrome [38]. We chose a dose of 10 mg/kg, since this is the minimum dose needed to detect the compound in biological samples by the chromatographic method.

The area under the plasma-concentration–time curve (AUC) showed significant differences between *Abcg2*<sup>-/-</sup> and wild-type mice from 20 min to 120 min post-administration (Figure 2), being, in *Abcg2*<sup>-/-</sup> mice, almost 2-fold higher than in the wild-type counterparts ( $1.29 \pm 0.11$   $\mu$ G·h/mL vs.  $0.72 \pm 0.05$   $\mu$ G·h/mL;  $p = 0.045$ ). Statistically significant differences were also found at the sampling time points of 45 min ( $0.39 \pm 0.24$   $\mu$ g/mL in wild-type mice vs.  $1.02 \pm 0.26$   $\mu$ g/mL in *Abcg2*<sup>-/-</sup> mice;  $p = 0.01$ ) and 60 min post-

administration ( $0.40 \pm 0.13 \mu\text{g/mL}$  in wild-type mice vs.  $0.85 \pm 0.50 \mu\text{g/mL}$  in  $\text{Abcg2}^{-/-}$  mice;  $p = 0.02$ ).

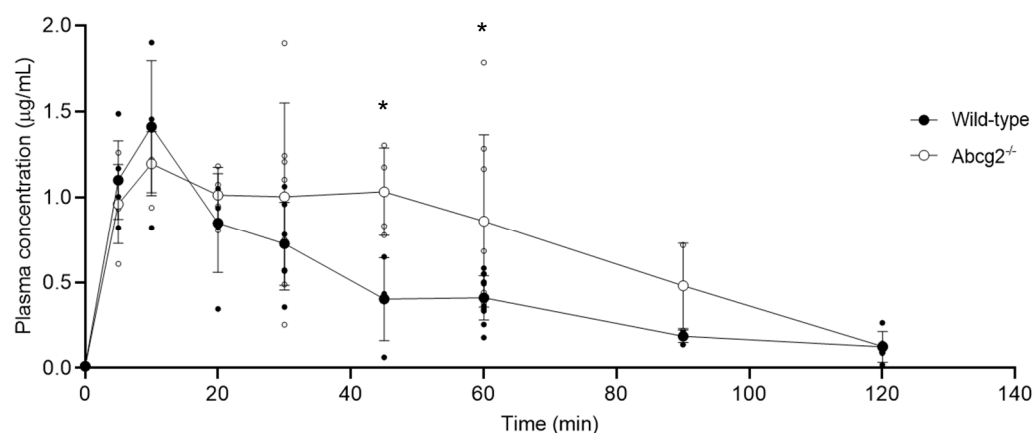


**Figure 2.** Plasma concentration after intraperitoneal administration of lumichrome (10 mg/kg) to wild-type and  $\text{Abcg2}^{-/-}$  male mice ( $n = 3-10$ ). Plasma samples were collected at 5, 10, 20, 30, 45, 60, 90 and 120 min. Concentration of lumichrome was determined by HPLC analysis. Results are presented as individual data and mean  $\pm$  S.D. (\*)  $p \leq 0.05$ : significant differences between both groups of mice.

In order to further study the role of ABCG2 in the biodistribution and elimination of lumichrome, concentrations of lumichrome were analyzed in the following tissues: liver, kidney, small intestine, small intestine content, spleen, brain and testis 60 min after intraperitoneal administration at a dose of 10 mg/kg (Figure 3).

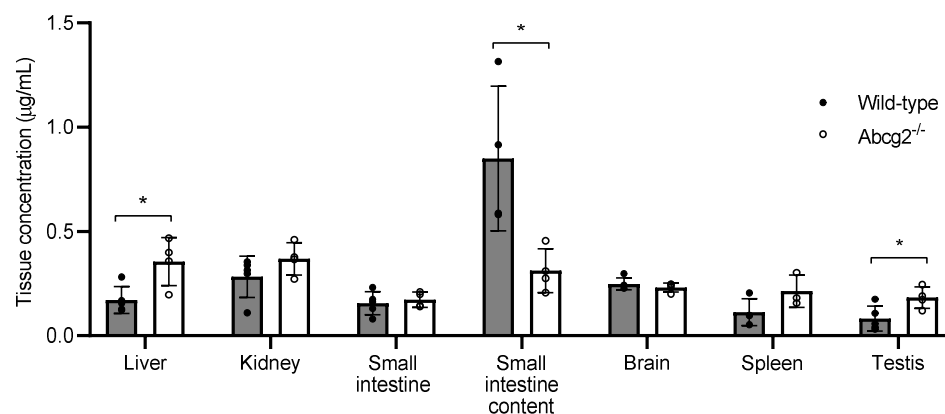


**Figure 3.** Tissue concentration of lumichrome in wild-type and  $\text{Abcg2}^{-/-}$  male mice 1 h after intraperitoneal administration of lumichrome at 10 mg/kg ( $n = 4-5$ ). Results are presented as individual data and mean  $\pm$  S.D. (\*)  $p \leq 0.05$ : significant differences between both groups of mice.

Lumichrome was widely distributed in all organs analyzed. Although at 60 min post-administration, plasma levels were 2.1-fold higher in  $\text{Abcg2}^{-/-}$  mice compared with their wild-type counterparts (Figure 2), lumichrome concentrations in small intestine content retrieved from wild-type mice were 2.7-fold higher than in  $\text{Abcg2}^{-/-}$  mice ( $0.85 \pm 0.35 \mu\text{g/mL}$  vs.  $0.31 \pm 0.11 \mu\text{g/mL}$ ). These results show that  $\text{Abcg2}$  mediates the excretion of lumichrome into the intestinal lumen, contributing to its elimination.

Additionally, statistically significant differences in concentrations between both types of animals were found in the liver and testis ( $p = 0.02$  and  $p = 0.03$ , respectively) (Figure 3). The liver and testis of  $\text{Abcg2}^{-/-}$  mice showed a 2.3-fold higher accumulation of lumichrome compared with wild-type mice ( $0.34 \pm 0.12 \mu\text{g/mL}$  vs.  $0.15 \pm 0.07 \mu\text{g/mL}$  and  $0.18 \pm 0.05 \mu\text{g/mL}$  vs.  $0.08 \pm 0.06 \mu\text{g/mL}$ , respectively).

These results demonstrate that lumichrome is an *in vivo* substrate of the ABCG2 transporter and it affects plasma concentrations and tissue distribution of lumichrome.

### 2.3. Secretion of Lumichrome into Milk in Wild-Type and *Abcg2*<sup>-/-</sup> Lactating Female Mice

To evaluate whether *Abcg2* is involved in the secretion of lumichrome into milk, 10 mg/kg of this compound was administered intraperitoneally to lactating wild-type and *Abcg2*<sup>-/-</sup> lactating female mice. Blood and milk samples were collected 30 min after administration.

Similar plasma levels (Figure 4A) were found in wild-type and *Abcg2*<sup>-/-</sup> mice ( $0.31 \pm 0.06 \mu\text{g/mL}$  vs.  $0.28 \pm 0.10 \mu\text{g/mL}$ , respectively). Conversely, accumulation of lumichrome in milk from wild-type mice (Figure 4B) was 4.1-fold higher in comparison with *Abcg2*<sup>-/-</sup> mice ( $1.75 \pm 0.73 \mu\text{g/mL}$  vs.  $0.43 \pm 0.18 \mu\text{g/mL}$ ;  $p < 0.01$ ). In addition, the milk-to-plasma ratio of lumichrome (Figure 4C) in wild-type mice was almost 3.7-fold higher than in *Abcg2*<sup>-/-</sup> mice ( $5.54 \pm 1.84 \mu\text{g/mL}$  vs.  $1.51 \pm 0.35 \mu\text{g/mL}$ ;  $p < 0.01$ ). These results reveal that *Abcg2* plays an important role in the active secretion of lumichrome into milk, absolutely confirming its *in vivo* interaction with the transporter.

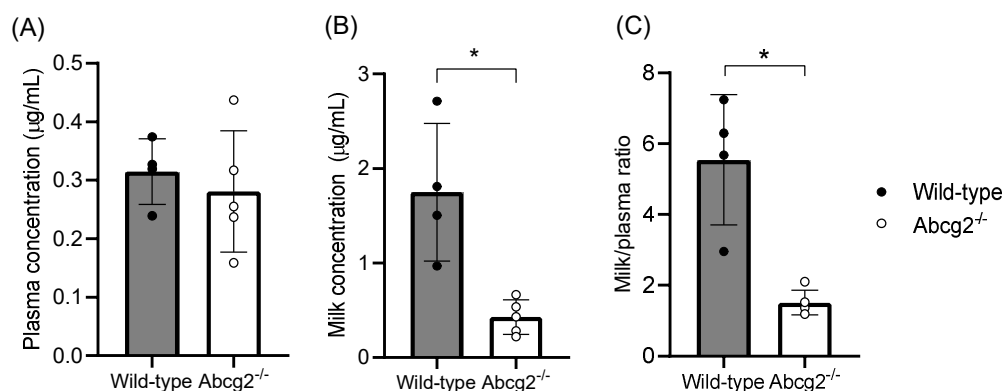


**Figure 4.** Plasma and milk concentrations and milk-to-plasma ratios of lumichrome in wild-type and *Abcg2*<sup>-/-</sup> female lactating mice after intraperitoneal administration of lumichrome at a dose of 10 mg/kg body weight ( $n = 4-5$ ). Plasma and milk samples were collected 30 min after intraperitoneal administration and concentrations were determined by HPLC. Results are presented as individual data and mean  $\pm$  S.D. (\*)  $p \leq 0.05$ : significant differences between both groups of mice.

### 3. Discussion

Lumichrome is an active derivative of riboflavin with relevant cytotoxic and prooxidant activities. Owing to the relationship between biological action and bioavailability, it is crucial to study the pharmacokinetics and systemic exposure of lumichrome and whether it is influenced by the presence of the efflux transporter ABCG2.

Accordingly, this study shows, for the first time, the *in vitro* interaction of lumichrome with the murine *Abcg2* and human ABCG2 and how murine *Abcg2* affects plasma levels, tissue accumulation and milk secretion of lumichrome.

*In vitro* transepithelial transport assays showed that lumichrome is efficiently transported by murine and human variants of the ABCG2 transporter, as well as other endogenous compounds like riboflavin [37]. The differences observed between murine and human ABCG2 transduced subclones correlated with the ones obtained for other ABCG2 substrates such as meloxicam [39] and albendazole sulphoxide [40], which could be attributed to a lower affinity with the compound of the human variant or a lower expression of the transporter in the aforementioned subclone [41].

In order to assess whether the *in vitro* results could be extrapolated to the *in vivo* situation, the concentration of lumichrome was determined in plasma and several tissues from wild-type and *Abcg2*<sup>-/-</sup> male mice after its intraperitoneal administration at a dose of 10 mg/kg. Although we cannot discount the possibility that the estimation of lumichrome

concentration might be affected by the degradation of endogenous riboflavin, the higher plasma  $AUC_{20-120 \text{ min}}$  in *Abcg2*<sup>-/-</sup> mice than in wild-type mice supports the idea that *Abcg2* contributes to lumichrome elimination (Figure 2), as was the case for riboflavin [37]. Therefore, any changes in *Abcg2* activity may alter the rate of elimination of lumichrome. This could have an impact on the success of its therapeutic use, such as in the case of photodynamic therapy, since lumichrome may be one of the photosensitizers chosen for the treatment of skin cancer and other diseases [42], for which systemic levels are therapeutically relevant. Changes in ABCG2 expression or functionality may alter the bioavailability and pharmacokinetics of ABCG2 substrates [2,43], potentially affecting their effects. This could be the case for lumichrome. Alterations in ABCG2 activity may be due to known genetic single nucleotide polymorphisms (SNPs), such as Q141K, which leads to a dysfunction of the transporter and has a high incidence rate among the Asian population [44]. Additionally, some natural [45] and dietary compounds including soy isoflavones [46,47] or flaxseed [48], and the coadministration of several drugs currently used in the treatment of human pathologies [49–51] may also decrease the activity of the transporter.

Regarding tissue distribution, our results show that lumichrome was distributed in all organs analyzed (Figure 3). The higher concentration of lumichrome in small intestine content retrieved from wild-type mice than from *Abcg2*<sup>-/-</sup> mice ( $0.85 \pm 0.35 \mu\text{g/mL}$  vs.  $0.31 \pm 0.11 \mu\text{g/mL}$ ) confirms that *Abcg2* contributes to lumichrome elimination. These results indicate that differences in concentrations in the intestinal lumen may be due to changes in *Abcg2* activity which may have consequences for the potential use of this compound in colorectal cancer [31]. For instance, in this case, a decreased concentration of lumichrome in the intestine, potentially due to intestinal ABCG2 inhibition by dietary compounds, may result in unsuccessful chemotherapy.

In relation to the liver and testis, *Abcg2*<sup>-/-</sup> mice showed a 2.3-fold-higher lumichrome accumulation compared with their wild-type counterparts in both organs ( $0.34 \pm 0.12 \mu\text{g/mL}$  vs.  $0.15 \pm 0.07 \mu\text{g/mL}$  and  $0.18 \pm 0.05 \mu\text{g/mL}$  vs.  $0.08 \pm 0.06 \mu\text{g/mL}$ , respectively), which may be a reflection of plasma differences. Even so, these divergences indicate that changes in the activity of the transporter can affect the levels of lumichrome in these organs and, therefore, its cytotoxic effect in a potential use of this compound against liver cancer cells [31].

To study milk secretion of lumichrome, *in vivo* assays with wild-type and *Abcg2*<sup>-/-</sup> female mice were performed. After the intraperitoneal administration of lumichrome at a dose of 10 mg/kg, similar plasma levels were found in both groups of mice ( $0.31 \pm 0.06 \mu\text{g/mL}$  vs.  $0.28 \pm 0.10 \mu\text{g/mL}$ , respectively). Notwithstanding, accumulation of lumichrome in milk (Figure 4B) and milk-to-plasma ratio (Figure 4C) from wild-type mice was higher in comparison with *Abcg2*<sup>-/-</sup> mice ( $1.75 \pm 0.73 \mu\text{g/mL}$  vs.  $0.43 \pm 0.18 \mu\text{g/mL}$ ;  $p < 0.01$  and  $5.54 \pm 1.84 \mu\text{g/mL}$  vs.  $1.51 \pm 0.35 \mu\text{g/mL}$ ;  $p < 0.01$ , respectively).

Higher concentrations of *Abcg2* substrates in milk of wild-type compared with *Abcg2*<sup>-/-</sup> mice were also observed after the administration of other natural substrates such as riboflavin [37], biotin [37], bile acids [52] or melatonin and its metabolites [53]. It has also been shown that the endogenous concentration of riboflavin in milk of wild-type mice was 63-fold higher than in the *Abcg2*<sup>-/-</sup> counterpart [37]. Comparing these results with the ones obtained for lumichrome administration, it can be stated that ABCG2 transports riboflavin more efficiently than lumichrome. These differences may be related to the fact that ABCG2 transports polar molecules more efficiently than non-polar ones [54]. In fact, riboflavin has a ribityl side chain which enwidens its topological polar surface area compared with lumichrome ( $155\text{\AA}^2$  vs.  $84\text{\AA}^2$ , respectively) [55,56].

Although the transport of lumichrome may be mediated by solute carrier (SLC) transporters [57–59], the main ABC efflux transporter upregulated during lactation in the mammary gland is ABCG2, which corroborates that, unequivocally, *Abcg2* plays a major role in the milk secretion of lumichrome, confirming the fact that lumichrome is an ABCG2 substrate. Compensatory changes in the expression of genes coding for proteins involved



in transport in the *Abcg2*<sup>-/-</sup> mice that could affect lumichrome biodistribution cannot be completely excluded. However, indications for such disturbing effects in previous studies have never been shown [60–62].

Changes in ABCG2 expression alter the concentration of ABCG2 substrates secreted into milk [6,53], including lumichrome, as we now report. Since this molecule affects sensorial properties of milk [34], any alteration in the transporter can change levels of lumichrome in milk, therefore potentially affecting milk quality [36].

In conclusion, our results support an important interaction between lumichrome and the ABCG2 transporter. This study shows, for the first time, that lumichrome is an *in vitro* substrate of murine and human variants of ABCG2. Furthermore, *in vivo* assays showed that *Abcg2* actively participates in bioavailability, tissue distribution and secretion of lumichrome into milk.

## 4. Materials and Methods

### 4.1. Chemicals

Lumichrome, mitoxantrone dihydrochloride and Lucifer Yellow were purchased from Sigma-Aldrich (St. Louis, MO, USA). Ko143 and albendazole-2-amino sulfone were acquired from Tocris (Bristol, UK) and LGC Standards (Teddington, Middlesex, UK), respectively. For *in vivo* assays, isoflurane (Isovet<sup>®</sup>, Isle Of Wight, UK) was obtained from B. Braun VetCare (Barcelona, Spain), oxytocin (Falcipart) from SYVA (León, Spain) and heparin (ROVI<sup>®</sup>, Madrid, Spain) from Laboratorios Farmacéuticos ROVI, S.A. (Madrid, Spain).

### 4.2. Cell Cultures

For *in vitro* assays, the polarized cell line Madin-Darby canine kidney (MDCK-II) and their murine *Abcg2* and human ABCG2 transduced subclones, which were previously generated [63,64] and provided by A.H. Schinkel from the Netherlands Cancer Institute (Amsterdam, The Netherlands), were used.

Cell culture conditions have been previously described [65]. Briefly, cells were cultured in Dulbecco's modified Eagle's medium (DMEM) supplemented with GlutaMAX<sup>™</sup> (Life Technologies, Paisley, UK), penicillin (50 units/mL) and streptomycin (50 µg/mL) (Life Technologies, Grand Island, NY, USA) and 10% (*v/v*) fetal bovine serum (MP Biomedicals, Solon, OH, USA), at 37 °C in an atmosphere with 5% CO<sub>2</sub>. Cells were trypsinized every 3 to 4 days for subculturing, when a subconfluent state was reached.

### 4.3. Transcellular Transport Assays

Transcellular transport assays were performed as previously described [66], with minor modifications (Figure S1). Transduced MDCK-II cells were seeded as a monolayer on microporous membrane filters (3.0 µm pore size, 24 mm diameter; Transwell<sup>®</sup> 3414; Costar, Corning, NY, USA) at a density of 1.0 × 10<sup>6</sup> cells/well. Cells were grown for three days with daily medium replacement.

During the experiment, quality controls were performed in terms of monolayer tightness at the beginning and end of the assay using Millicell<sup>®</sup>ERS (Millipore, Burlington, MA, USA), and monolayer confluence was tested at the end of the experiment by means of Lucifer Yellow permeability [67]. Transport proficiency was simultaneously checked by testing a typical ABCG2 substrate (danofloxacin 10 µM) (Table S1).

Two hours before the start of the assay, medium at both the apical and basolateral side of the monolayer was replaced with 2 mL of prewarmed Opti-MEM medium (Life Technologies, Paisley, UK), either with or without the inhibitor Ko143 (1 µM) [66] (to verify that the potential transport was specifically due to ABCG2). The experiment began (*t* = 0 h) by replacing the medium of both compartments with fresh Opti-MEM medium with or without inhibitor and containing 10 µM lumichrome. Cells were incubated at 37 °C in an atmosphere with 5% CO<sub>2</sub> and 100 µL aliquots were taken at 1, 2 and 3 h on the opposite side to where lumichrome had been added. This volume was replaced with fresh Opti-MEM medium. Finally, at *t* = 4 h 600 µL aliquots were taken from the apical and basal

compartments of each well. All samples were stored at  $-20\text{ }^{\circ}\text{C}$  until being analyzed by high-performance liquid chromatography (HPLC), as described below.

Lumichrome appearance in the opposite compartment is presented as the fraction of total compound added at the beginning of the experiment and expressed as percentage. The relative efflux transport ratio was calculated as the basal to apical directed transport percentage divided by the apical to basal directed transport percentage at 4 h.

#### 4.4. Animals

Animals were handled according to institutional and ARRIVE guidelines complying with European legislation (2010/63/EU). Experimental procedures were approved by the Animal Care and Use Committee of the University of León and the Junta de Castilla y León (ULE\_010\_2021). *Abcg2<sup>-/-</sup>* and wild-type mice were used, all of >99% FVB/N genetic background, generated and kindly supplied by A. H. Schinkel (The Netherlands Cancer Institute) [68].

All animals, which were aged from 9 to 14 weeks and weighed 30 g, were kept in a temperature-controlled environment with a cycle of 12 h of light and 12 h of darkness and received a standard diet and water ad libitum.

##### 4.4.1. Plasma and Tissue Distribution

For in vivo assays, 10 mg/kg lumichrome, 200  $\mu\text{L}$  of compound solution [appropriate concentration in 6% (*v/v*) ethanol, 42% (*v/v*) polyethylene glycol 400 and 52% (*v/v*) saline solution] per 30 g of body weight, was intraperitoneally administrated.

Blood samples were collected at different time points (5, 10, 20, 30, 45, 60, 90 and 120 min) by cardiac puncture under anesthesia with isoflurane. Organs were harvested at the 60 min time point. All animals were euthanized by cervical dislocation at the end of the experimental procedure. Heparinized blood samples were centrifuged immediately at  $3000\times g$  for 15 min. Plasma and organs were stored at  $-20\text{ }^{\circ}\text{C}$  until HPLC analysis. Three to ten animals were used for each time point.

##### 4.4.2. Milk Secretion Experiments

Pups of approximately 10 days old were separated from their mothers four hours before the onset of the experiment. Lumichrome 10 mg/kg solution, prepared as described above, was administered intraperitoneally, at 200  $\mu\text{L}$  per 30 g of body weight. Milk secretion was stimulated by oxytocin (200  $\mu\text{L}$  of a 1 UI/mL solution), subcutaneously injected to lactating mice 10 min before sample collection. Then, 30 min after lumichrome administration, blood and milk samples from the mammary gland were collected by retro-orbital plexus puncture and gentle pinching around the nipple using capillaries, respectively, under anesthesia with isoflurane. Animals were euthanized by cervical dislocation at the end of the experiment. Four to five animals were used for each group.

Heparinized blood samples were centrifuged immediately at  $3000\times g$  for 15 min to obtain plasma. Milk and plasma were also stored at  $-20\text{ }^{\circ}\text{C}$  until HPLC analysis.

#### 4.5. High-Performance Liquid Chromatographic Analysis

Samples were analyzed in a chromatographic system, which consisted of a Waters 2695 separation module and a Waters 2998 UV photodiode array detector.

Lumichrome was determined as previously described [37], with minor modifications. Tissue samples were homogenized with a mixture of 50% water:50% methanol with 0.5% HCl; 1 mL of solution per 0.1 g of organ was used. To each 100  $\mu\text{L}$  of plasma, milk or tissue homogenate, 10  $\mu\text{L}$  of an albendazole-2-aminosulfone solution (100  $\mu\text{g}/\text{mL}$ ) was added as an internal standard and 400  $\mu\text{L}$  of acetonitrile was also added in order to precipitate proteins. After 10 min of being horizontally vortexed, samples were centrifuged at  $10,500\times g$  for 10 min at  $4\text{ }^{\circ}\text{C}$ . Supernatants were evaporated to dryness at  $40\text{ }^{\circ}\text{C}$  under a stream of nitrogen. Samples were reconstituted in 100  $\mu\text{L}$  of cold methanol and injected



into the HPLC system. However, samples for in vitro assays were directly injected into the HPLC system.

The chromatographic system used for sample analysis consisted of a Waters 2695 separation module and a Waters 2998 UV photodiode array detector. Separation of samples was performed on an analytical reversed-phase column (5  $\mu\text{m}$  particle size, 250  $\times$  4.6 mm, EVO C18 100  $\text{\AA}$ , Phenomenex<sup>®</sup>, Torrance, CA, USA). The mobile phase used for in vitro samples was trifluoroacetic acid 0.04%:methanol (40:60), whereas for in vivo samples, it was ammonium acetate 25 mM (pH 5):acetonitrile (85:15). In both cases, the flow rate was set to 1.00 mL/min and UV absorbance was measured at 260.3 nm.

Standard samples of lumichrome in the appropriate drug-free matrix were prepared yielding a concentration range of 0.0195–5  $\mu\text{g}/\text{mL}$  for culture, plasma and tissue samples and 0.078–2.5  $\mu\text{g}/\text{mL}$  for milk samples. Coefficients of correlation for culture and milk samples were above 0.99, whereas in plasma samples they ranged between 0.98 and 0.99, and in tissue samples between 0.94 and 0.99.

The limit of quantification (LOQ) and limit of detection (LOD) were calculated as described by Taverniers et al. [69]. LOQ was 0.008  $\mu\text{g}/\text{mL}$  and LOD 0.003  $\mu\text{g}/\text{mL}$  for cell culture samples; LOQ was 0.042  $\mu\text{g}/\text{mL}$  and LOD 0.022  $\mu\text{g}/\text{mL}$  for plasma samples; LOQ was 0.046  $\mu\text{g}/\text{mL}$  and LOD 0.023  $\mu\text{g}/\text{mL}$  for milk samples and for tissues, LOQ was 0.019–0.061  $\mu\text{g}/\text{mL}$  and LOD 0.011–0.040  $\mu\text{g}/\text{mL}$ .

#### 4.6. Statistical Analysis

Statistical analysis was carried out using SPSS Statistics software (v. 26.0; IBM, Armonk, New York, NY, USA). The Shapiro–Wilk test was performed to check normal distribution. Comparison between groups was made applying the two-tailed unpaired Student's t-test or the Mann–Whitney U test to normally or not-normally distributed data, respectively.  $p$  value  $\leq 0.05$  indicates statistically significant differences between groups.

**Supplementary Materials:** The following supporting information can be downloaded at: <https://www.mdpi.com/article/10.3390/ijms25189884/s1>.

**Author Contributions:** Conceptualization, A.M.-G., A.I.Á. and G.M.; methodology, A.M.-G., L.Á.-F., E.B.-P. and G.M.; data curation and writing—original draft preparation, A.M.-G.; writing—review and editing, G.M.; validation, resources and project administration, G.M.; supervision and funding acquisition, A.I.Á. and G.M. All authors have read and agreed to the published version of the manuscript.

**Funding:** The authors declare that financial support was received for the research, authorship and/or publication of this article. This work was supported by the research project PID2021-125660OB-I00 (MCIN/AEI/10.13039/501100011033/FEDER “Una manera de hacer Europa”) and by predoctoral grants (FPU18/01559 grant to E.B.-P, FPU19/04169 grant to L.Á.-F) from the Spanish Ministry of Education, Culture and Sport, and ULE2022 grant to A.M.-G from the University of León.

**Institutional Review Board Statement:** The animal study protocol was approved by the Animal Care and Use Committee of the University of León and the Junta de Castilla y León (ULE\_010\_2021, approved on 6 July 2021). Mice were housed and handled complying with institutional and ARRIVE guidelines and European legislation (EU Directive 2010/63/EU for animal experiments).

**Informed Consent Statement:** Not applicable.

**Data Availability Statement:** The data supporting the reported results are available from the corresponding author upon request.

**Acknowledgments:** The authors thank A.H. Schinkel (The Netherlands Cancer Institute, Amsterdam, The Netherlands) who kindly provided parental MDCK–II cells and their murine Abcg2 and ABCG2–transduced subclones, as well as Abcg2 knockout mice.

**Conflicts of Interest:** The authors declare no conflicts of interest. The funders had no role in the design of the study; in the collection, analyses, or interpretation of data; in the writing of the manuscript; or in the decision to publish the results.

## References

1. Vlaming, M.L.; Lagas, J.S.; Schinkel, A.H. Physiological and pharmacological roles of ABCG2 (BCRP): Recent findings in Abcg2 knockout mice. *Adv. Drug Deliv. Rev.* **2008**, *61*, 14–25. [[CrossRef](#)] [[PubMed](#)]
2. Horsey, A.J.; Cox, M.H.; Sarwat, S.; Kerr, I.D. The multidrug transporter ABCG2: Still more questions than answers. *Biochem. Soc. Trans.* **2016**, *44*, 824–830. [[CrossRef](#)]
3. Khunweeraphong, N.; Szöllösi, D.; Stockner, T.; Kuchler, K. The ABCG2 multidrug transporter is a pump gated by a valve and an extracellular lid. *Nat. Commun.* **2019**, *10*, 1–14. [[CrossRef](#)] [[PubMed](#)]
4. Kukal, S.; Guin, D.; Rawat, C.; Bora, S.; Mishra, M.K.; Sharma, P.; Paul, P.R.; Kanojia, N.; Grewal, G.K.; Kukreti, S.; et al. Multi-drug Efflux Transporter ABCG2: Expression and Regulation. *Cell. Mol. Life Sci.* **2021**, *78*, 6887–6939. [[CrossRef](#)]
5. Qi, X.; Chen, H.; Guan, K.; Wang, R.; Ma, Y. Anti-hyperuricemic and nephroprotective effects of whey protein hydrolysate in potassium oxonate induced hyperuricemic rats. *J. Sci. Food Agric.* **2021**, *101*, 4916–4924. [[CrossRef](#)] [[PubMed](#)]
6. García-Lino, A.M.; Álvarez-Fernández, I.; Blanco-Paniagua, E.; Merino, G.; Álvarez, A.I. Transporters in the Mammary Gland—Contribution to Presence of Nutrients and Drugs into Milk. *Nutrients* **2019**, *11*, 2372. [[CrossRef](#)]
7. Prukala, D.; Sikorska, E.; Koput, J.; Khmelinskii, I.; Karolczak, J.; Gierszewski, M.; Sikorski, M. Acid-Base Equilibriums of Lu-michrome and Its 1-Methyl, 3-Methyl, and 1,3-Dimethyl Derivatives. *J. Phys. Chem. A* **2012**, *116*, 7474–7490. [[CrossRef](#)]
8. Ahmad, I.; Fasihullah, Q.; Vaid, F.H.M. A Study of Simultaneous Photolysis and Photoaddition Reactions of Riboflavin in Aqueous Solution. *J. Photochem. Photobiol. B Biol.* **2004**, *75*, 13–20. [[CrossRef](#)]
9. Huang, R.; Kim, H.J.; Min, D.B. Photosensitizing Effect of Riboflavin, Lumiflavin, and Lumichrome on the Generation of Volatiles in Soy Milk. *J. Agric. Food Chem.* **2006**, *54*, 2359–2364. [[CrossRef](#)]
10. Remucal, C.K.; McNeill, K. Photosensitized Amino Acid Degradation in the Presence of Riboflavin and Its Derivatives. *Environ. Sci. Technol.* **2011**, *45*, 5230–5237. [[CrossRef](#)]
11. Bergh, V.J.V.; Tønnesen, H.H. Interaction between the photosensitizer lumichrome and human serum albumin: Effect of excipients. *Pharm. Dev. Technol.* **2016**, *22*, 992–1000. [[CrossRef](#)] [[PubMed](#)]
12. Hardwick, C.C.; Herivel, T.R.; Hernandez, S.C.; Ruane, P.H.; Goodrich, R.P. Separation, Identification and Quantification of Riboflavin and Its Photoproducts in Blood Products Using High-performance Liquid Chromatography with Fluorescence Detection: A Method to Support Pathogen Reduction Technology. *Photochem. Photobiol.* **2004**, *80*, 609–615. [[PubMed](#)]
13. Jana, R.; Gautam, R.K.; Bapli, A.; Seth, D. Photodynamics of Biological Active Flavin in the Presence of Zwitterionic Surfactants. *Spectrochim. Acta Part A Mol. Biomol. Spectrosc.* **2022**, *264*, 120304. [[CrossRef](#)]
14. Oka, M.; McCormick, D.B. Urinary Lumichrome-Level Catabolites of Riboflavin are due to Microbial and Photochemical Events and not Rat Tissue Enzymatic Cleavage of the Ribityl Chain. *J. Nutr.* **1985**, *115*, 496–499. [[CrossRef](#)]
15. Hamada, K.; Sasaki, M.; Yoshimura, K. Two New Types of Riboflavin-Decomposing Bacteria Isolated from Human Feces. *J. Vitaminol.* **1956**, *2*, 307–315. [[CrossRef](#)]
16. Yamamoto, K.; Asano, Y. Efficient Production of Lumichrome by *Microbacterium* sp. Strain TPU 3598. *Appl. Environ. Microbiol.* **2015**, *81*, 7360–7367. [[CrossRef](#)] [[PubMed](#)]
17. Foster, J.W. Microbiological Aspects of Riboflavin: III. Oxidation Studies with *Pseudomonas Riboflavina*. *J. Bacteriol.* **1944**, *48*, 97–111. [[CrossRef](#)]
18. Alves, A.J.S.; Pereira, J.A.; Dethoup, T.; Cravo, S.; Mistry, S.; Silva, A.M.S.; Pinto, M.M.M.; Kijjoa, A. A New Meroterpene, A New Benzofuran Derivative and Other Constituents from Cultures of the Marine Sponge-Associated Fungus *Acremonium persicinum* KUFA 1007 and Their Anticholinesterase Activities. *Mar. Drugs* **2019**, *17*, 379. [[CrossRef](#)]
19. Kino, K.; Nakatsuma, A.; Nochi, H.; Kiriya, Y.; Kurita, T.; Kobayashi, T.; Miyazawa, H. Commentary on the Phototoxicity and Absorption of Vitamin B2 and Its Degradation Product, Lumichrome. *Pharm. Anal. Acta* **2015**, *6*, 8–10.
20. Kino, K.; Kobayashi, T.; Arima, E.; Komori, R.; Kobayashi, T.; Miyazawa, H. Photoirradiation products of flavin derivatives, and the effects of photooxidation on guanine. *Bioorg. Med. Chem. Lett.* **2009**, *19*, 2070–2074. [[CrossRef](#)]
21. Seng, F.; Ley, K. A New Synthesis of Lumichrome. *Angew. Chem. Int. Ed. Engl.* **1972**, *11*, 1010–1011. [[CrossRef](#)]
22. Huang, R.; Choe, E.; Min, D. Effects of Riboflavin Photosensitized Oxidation on the Volatile Compounds of Soymilk. *J. Food Sci.* **2004**, *69*, C733–C738. [[CrossRef](#)]
23. Ahmad, I.; Anwar, Z.; Sheraz, M.A.; Ahmed, S.; Khattak, S.U.R. Stability-indicating spectrofluorimetric method for the assay of riboflavin and photoproducts: Kinetic applications. *Luminescence* **2018**, *33*, 1070–1080. [[CrossRef](#)] [[PubMed](#)]
24. Marchena, M.; Gil, M.; Martín, C.; Organero, J.A.; Sanchez, F.; Douhal, A. Stability and Photodynamics of Lumichrome Structures in Water at Different pHs and in Chemical and Biological Caging Media. *J. Phys. Chem. B* **2011**, *115*, 2424–2435. [[CrossRef](#)]
25. Cunningham, O.; Gore, M.G.; Mantle, T.J. Initial-Rate Kinetics of the Flavin Reductase Reaction Catalysed by Human Biliverdin-IX $\beta$  Reductase (BVR-B). *Biochem. J.* **2000**, *345*, 393–399. [[CrossRef](#)]
26. Fieschi, F.; Nivière, V.; Frier, C.; Décout, J.-L.; Fontecave, M. The Mechanism and Substrate Specificity of the NADPH:Flavin Oxidoreductase from *Escherichia coli*. *J. Biol. Chem.* **1995**, *270*, 30392–30400. [[CrossRef](#)] [[PubMed](#)]
27. Shalloe, F.; Elliott, G.; Ennis, O.; Mantle, T.J. Evidence that biliverdin-IX $\beta$  reductase and flavin reductase are identical. *Biochem. J.* **1996**, *316*, 385–387. [[CrossRef](#)]
28. Said, H.M.; Ortiz, A.; Ma, T.Y.; McCloud, E. Riboflavin uptake by the human-derived liver cells Hep G2: Mechanism and regulation. *J. Cell. Physiol.* **1998**, *176*, 588–594. [[CrossRef](#)]

29. Grønlien, K.G.; Pedersen, M.E.; Rønning, S.B.; Solberg, N.T.; Tønnesen, H.H. Tuning of 2D Cultured Human Fibroblast Behavior Using Lumichrome Photocrosslinked Collagen Hydrogels. *Mater. Today Commun.* **2022**, *31*, 103635. [[CrossRef](#)]
30. Chantarawong, W.; Kuncharoen, N.; Tanasupawat, S.; Chanvorachote, P. Lumichrome Inhibits Human Lung Cancer Cell Growth and Induces Apoptosis via a p53-Dependent Mechanism. *Nutr. Cancer* **2019**, *71*, 1390–1402. [[CrossRef](#)]
31. Etu, S.F.; Alqanthan, A.; Qais, N. 5,10-Dihydro-7,8-Dimethyl Alloxazine as an Anticancer Agent from Lumichrome of Riboflavin. *J. Drug Des. Dev.* **2021**, *2*, 44–48.
32. Tan, D.; Ma, A.; Wang, S.; Zhang, Q.; Jia, M.; Kamal-Eldin, A.; Wu, H.; Chen, G. Effects of the Oxygen Content and Light Intensity on Milk Photooxidation Using Untargeted Metabolomic Analysis. *J. Agric. Food Chem.* **2021**, *69*, 7488–7497. [[CrossRef](#)] [[PubMed](#)]
33. Tan, S.; Li, Q.; Guo, C.; Chen, S.; Kamal-Eldin, A.; Chen, G. Reveal the mechanism of hepatic oxidative stress in mice induced by photo-oxidation milk using multi-omics analysis techniques. *J. Adv. Res.* **2024**. [[CrossRef](#)] [[PubMed](#)]
34. Fracassetti, D.; Limbo, S.; D'incecco, P.; Tirelli, A.; Pellegrino, L. Development of a HPLC method for the simultaneous analysis of riboflavin and other flavin compounds in liquid milk and milk products. *Eur. Food Res. Technol.* **2018**, *244*, 1545–1554. [[CrossRef](#)]
35. Min, D.B.; Boff, J.M. Chemistry and Reaction of Singlet Oxygen in Foods. *Compr. Rev. Food Sci. Food Saf.* **2002**, *1*, 58–72. [[CrossRef](#)]
36. Keim, J.P.; Daza, J.; Beltrán, I.; Balocchi, O.A.; Pulido, R.G.; Sepúlveda-Varas, P.; Pacheco, D.; Berthiaume, R. Milk Production Responses, Rumen Fermentation, and Blood Metabolites of Dairy Cows Fed Increasing Concentrations of Forage Rape (*Brassica Napus* Ssp. *Biennis*). *J. Dairy Sci.* **2020**, *103*, 9054–9066. [[CrossRef](#)]
37. van Herwaarden, A.E.; Wagenaar, E.; Merino, G.; Jonker, J.W.; Rosing, H.; Beijnen, J.H.; Schinkel, A.H. Multidrug Transporter ABCG2/Breast Cancer Resistance Protein Secretes Riboflavin (Vitamin B2) into Milk. *Mol. Cell. Biol.* **2007**, *27*, 1247–1253. [[CrossRef](#)]
38. Liu, C.; Cao, Z.; Zhang, W.; Tickner, J.; Qiu, H.; Wang, C.; Chen, K.; Wang, Z.; Tan, R.; Dong, S.; et al. Lumichrome inhibits osteoclastogenesis and bone resorption through suppressing RANKL-induced NFAT activation and calcium signaling. *J. Cell. Physiol.* **2018**, *233*, 8971–8983. [[CrossRef](#)]
39. Garcia-Lino, A.M.; Blanco-Paniagua, E.; Astorga-Simon, E.N.; Alvarez-Fernandez, L.; Garcia-Mateos, D.; Alvarez-Fernandez, I.; Alvarez, A.I.; Merino, G. Abcg2 transporter affects plasma, milk and tissue levels of meloxicam. *Biochem. Pharmacol.* **2020**, *175*, 113924. [[CrossRef](#)]
40. Blanco-Paniagua, E.; Álvarez-Fernández, L.; Garcia-Lino, A.M.; Álvarez, A.I.; Merino, G. Secretion into Milk of the Main Metabolites of the Anthelmintic Albendazole Is Mediated by the ABCG2/BCRP Transporter. *Antimicrob. Agents Chemother.* **2022**, *66*, e0006222. [[CrossRef](#)]
41. Real, R.; Egido, E.; Pérez, M.; González-Lobato, L.; Barrera, B.; Prieto, J.G.; Álvarez, A.I.; Merino, G. Involvement of breast cancer resistance protein (BCRP/ABCG2) in the secretion of danofloxacin into milk: Interaction with ivermectin. *J. Veter. Pharmacol. Ther.* **2010**, *34*, 313–321. [[CrossRef](#)] [[PubMed](#)]
42. Insińska-Rak, M.; Sikorski, M.; Wolnicka-Glubisz, A. Riboflavin and Its Derivates as Potential Photosensitizers in the Photodynamic Treatment of Skin Cancers. *Cells* **2023**, *12*, 2304. [[CrossRef](#)] [[PubMed](#)]
43. Hira, D.; Terada, T. BCRP/ABCG2 and high-alert medications: Biochemical, pharmacokinetic, pharmacogenetic, and clinical implications. *Biochem. Pharmacol.* **2018**, *147*, 201–210. [[CrossRef](#)] [[PubMed](#)]
44. Polgar, O.; Robey, R.W.; E Bates, S. ABCG2: Structure, function and role in drug response. *Expert. Opin. Drug Metab. Toxicol.* **2007**, *4*, 1–15. [[CrossRef](#)] [[PubMed](#)]
45. Wu, C.; Lusvardi, S.; Hsiao, S.; Liu, T.; Li, Y.; Huang, Y.; Hung, T.; Chang, T.; Memorial, G. Licochalcone A Selectively Resensitizes ABCG2-Overexpressing Multidrug-Resistant Cancer Cells to Chemotherapeutic Drugs. *J. Nat. Prod.* **2020**, *83*, 1461–1472. [[CrossRef](#)]
46. Perez, M.; Otero, J.A.; Barrera, B.; Prieto, J.G.; Merino, G.; Alvarez, A.I. Inhibition of ABCG2/BCRP Transporter by Soy Isoflavones Genistein and Daidzein: Effect on Plasma and Milk Levels of Danofloxacin in Sheep. *Vet. J.* **2013**, *196*, 203–208. [[CrossRef](#)]
47. Gunes, Y.; Okyar, A.; Krajcsi, P.; Fekete, Z.; Ustuner, O. Modulation of monepantel secretion into milk by soy isoflavones. *J. Veter-Pharmacol. Ther.* **2022**, *46*, 185–194. [[CrossRef](#)]
48. Otero, J.A.; García-Mateos, D.; Alvarez-Fernández, I.; García-Villalba, R.; Espín, J.C.; Álvarez, A.I.; Merino, G. Flaxseed-enriched diets change milk concentration of the antimicrobial danofloxacin in sheep. *BMC Veter. Res.* **2018**, *14*, 14. [[CrossRef](#)]
49. Mao, Q.; Unadkat, J.D. Role of the Breast Cancer Resistance Protein (BCRP/ABCG2) in Drug Transport—An Update. *AAPS J.* **2014**, *17*, 65–82. [[CrossRef](#)]
50. Sabet, Z.; Vagiannis, D.; Budagaga, Y.; Zhang, Y.; Novotná, E.; Hanke, I.; Rozkoš, T.; Hofman, J. Talazoparib Does Not Interact with ABCB1 Transporter or Cytochrome P450s, but Modulates Multidrug Resistance Mediated by ABCB1 and ABCG2: An In Vitro and Ex Vivo Study. *Int. J. Mol. Sci.* **2022**, *23*, 14338. [[CrossRef](#)]
51. Sharma, S.; Mettu, V.S.; Prasad, B. Interplay of Breast Cancer Resistance Protein (Bcrp/Abcg2), Sex, and Fed State in Oral Pharmacokinetic Variability of Furosemide in Rats. *Pharmaceutics* **2023**, *15*, 542. [[CrossRef](#)] [[PubMed](#)]
52. Blazquez, A.M.G.; Macias, R.I.R.; Cives-Losada, C.; de la Iglesia, A.; Marin, J.J.G.; Monte, M.J. Lactation during cholestasis: Role of ABC proteins in bile acid traffic across the mammary gland. *Sci. Rep.* **2017**, *7*, 7475. [[CrossRef](#)] [[PubMed](#)]
53. Alvarez-Fernández, L.; Gomez-Gomez, A.; Haro, N.; García-Lino, A.M.; Álvarez, A.I.; Pozo, O.J.; Merino, G. ABCG2 Transporter Plays a Key Role in the Biodistribution of Melatonin and Its Main Metabolites. *J. Pineal Res.* **2023**, *74*, e12849. [[CrossRef](#)] [[PubMed](#)]
54. Egido, E.; Müller, R.; Li-Blatter, X.; Merino, G.; Seelig, A. Predicting Activators and Inhibitors of the Breast Cancer Resistance Protein (ABCG2) and P-Glycoprotein (ABCB1) Based on Mechanistic Considerations. *Mol. Pharm.* **2015**, *12*, 4026–4037. [[CrossRef](#)]

55. Riboflavin | C17H20N4O6 | CID 493570–PubChem. Available online: <https://pubchem.ncbi.nlm.nih.gov/compound/Riboflavin> (accessed on 10 March 2024).
56. Lumichrome | C12H10N4O2 | CID 5326566–PubChem. Available online: <https://pubchem.ncbi.nlm.nih.gov/compound/5326566> (accessed on 10 March 2024).
57. Fujimura, M.; Yamamoto, S.; Murata, T.; Yasujima, T.; Inoue, K.; Ohta, K.-Y.; Yuasa, H. Functional Characteristics of the Human Ortholog of Riboflavin Transporter 2 and Riboflavin-Responsive Expression of Its Rat Ortholog in the Small Intestine Indicate Its Involvement in Riboflavin Absorption. *J. Nutr.* **2010**, *140*, 1722–1727. [[CrossRef](#)]
58. Kubo, Y.; Miki, S.; Akanuma, S.; Hosoya, K. Ichi Riboflavin Transport Mediated by Riboflavin Transporters (RFVTs/SLC52A) at the Rat Outer Blood-Retinal Barrier. *Drug Metab. Pharmacokinet.* **2019**, *34*, 380–386. [[CrossRef](#)]
59. Patel, M.; Vadlapatla, R.K.; Pal, D.; Mitra, A.K. Molecular and Functional Characterization of Riboflavin Specific Transport System in Rat Brain Capillary Endothelial Cells. *Brain Res.* **2012**, *1468*, 1–10. [[CrossRef](#)]
60. Dallas, S.; Salphati, L.; Gomez-Zepeda, D.; Wanek, T.; Chen, L.; Chu, X.; Kunta, J.; Mezler, M.; Menet, M.-C.; Chasseigneaux, S.; et al. Generation and Characterization of a Breast Cancer Resistance Protein Humanized Mouse Model. *Mol. Pharmacol.* **2016**, *89*, 492–504. [[CrossRef](#)]
61. Agarwal, S.; Uchida, Y.; Mittapalli, R.K.; Sane, R.; Terasaki, T.; Elmquist, W.F. Quantitative Proteomics of Transporter Expression in Brain Capillary Endothelial Cells Isolated from P-Glycoprotein (P-Gp), Breast Cancer Resistance Protein (Bcrp), and P-Gp/Bcrp Knockout Mice. *Drug Metab. Dispos.* **2012**, *40*, 1164–1169. [[CrossRef](#)]
62. Lagas, J.S.; van Waterschoot, R.A.; Sparidans, R.W.; Wagenaar, E.; Beijnen, J.H.; Schinkel, A.H. Breast Cancer Resistance Protein and P-glycoprotein Limit Sorafenib Brain Accumulation. *Mol. Cancer Ther.* **2010**, *9*, 319–326. [[CrossRef](#)]
63. Jonker, J.W.; Brinkhuis, R.F.; Maliepaard, M.; Beijnen, J.H.; Schellens, J.H.M.; Schinkel, A.H. Role of Breast Cancer Resistance Protein in the Bioavailability and Fetal Penetration of Topotecan. *JNCI J. Natl. Cancer Inst.* **2000**, *92*, 1651–1656. [[CrossRef](#)] [[PubMed](#)]
64. Pavek, P.; Merino, G.; Wagenaar, E.; Bolscher, E.; Novotna, M.; Jonker, J.W.; Schinkel, A.H. Human Breast Cancer Resistance Protein: Interactions with Steroid Drugs, Hormones, the Dietary Carcinogen Transport of Cimetidine. *J. Pharmacol. Exp. Ther.* **2005**, *312*, 144–152. [[CrossRef](#)] [[PubMed](#)]
65. González-Lobato, L.; Real, R.; Herrero, D.; de la Fuente, A.; Prieto, J.G.; Marqués, M.M.; Álvarez, A.I.; Merino, G. Novel in Vitro Systems for Prediction of Veterinary Drug Residues in Ovine Milk and Dairy Products. *Food Addit. Contam.—Part A* **2014**, *31*, 1026–1037. [[CrossRef](#)] [[PubMed](#)]
66. Merino, G.; Jonker, J.W.; Wagenaar, E.; van Herwaarden, A.E.; Schinkel, A.H. The Breast Cancer Resistance Protein (BCRP/ABCG2) Affects Pharmacokinetics, Hepatobiliary Excretion, and Milk Secretion of the Antibiotic Nitrofurantoin. *Mol. Pharmacol.* **2005**, *67*, 1758–1764. [[CrossRef](#)]
67. Mahnke, H.; Ballent, M.; Baumann, S.; Imperiale, F.; von Bergen, M.; Lanusse, C.; Lifschitz, A.L.; Honscha, W.; Halwachs, S. The ABCG2 Efflux Transporter in the Mammary Gland Mediates Veterinary Drug Secretion across the Blood-Milk Barrier into Milk of Dairy Cows. *Drug Metab. Dispos.* **2016**, *44*, 700–708. [[CrossRef](#)]
68. Jonker, J.W.; Buitelaar, M.; Wagenaar, E.; van der Valk, M.A.; Scheffer, G.L.; Scheper, R.J.; Plösch, T.; Kuipers, F.; Elferink, R.P.J.O.; Rosing, H.; et al. The breast cancer resistance protein protects against a major chlorophyll-derived dietary phototoxin and protoporphyria. *Proc. Natl. Acad. Sci. USA* **2002**, *99*, 15649–15654. [[CrossRef](#)]
69. Taverniers, I.; De Loose, M.; Van Bockstaele, E. Trends in Quality in the Analytical Laboratory. II. Analytical Method Validation and Quality Assurance. *TrAC Trends Anal. Chem.* **2004**, *23*, 535–552. [[CrossRef](#)]

**Disclaimer/Publisher’s Note:** The statements, opinions and data contained in all publications are solely those of the individual author(s) and contributor(s) and not of MDPI and/or the editor(s). MDPI and/or the editor(s) disclaim responsibility for any injury to people or property resulting from any ideas, methods, instructions or products referred to in the content.